Mean-square nuclear charge radius of radioactive ^{144}Ce by laser spectroscopy

Y. Ishida
Department of Physics, Hiroshima University, Kagamiyama, Higashi-Hiroshima 739-8526, Japan

H. Iimura and S. Ichikawa
Nuclear Chemistry Laboratory, Japan Atomic Energy Research Institute, Tokai, Ibaraki 319-1195, Japan

T. Horiguchi
Department of Clinical Radiology, Hiroshima International University, Kurose 724-0695, Japan
(Received 5 October 1998)

The isotope shift of an optical transition ($\lambda = 534.93$ nm) in Ce^+ for radioactive ^{144}Ce has been measured by collinear laser-ion-beam spectroscopy as well as those of stable isotopes. The change in mean-square nuclear charge radius determined from the isotope shift is $\delta\langle r^2\rangle^{142,144} = 0.232(20)$ fm^2, and compared with the values from the reduced $E2$ transition probability and the theoretical predictions. [S0556-2813(99)02403-6]

PACS number(s): 21.10.Ft, 27.60.+j, 32.30.Jc

Precise and systematic studies of the isotope shift (IS) of optical transitions provide the information on changes in the mean-square nuclear charge radius (MSCR). That study in the region of light rare-earth elements is of interest because it gives an opportunity to investigate the effect of neutron shell closure at $N = 82$. Also, other nuclear structural changes are expected for the neutron-rich isotopes in this region [1]. Especially, it is well known that a drastic shape transition occurs between the neutron numbers of $N = 88$ and 90 in the isotopic chains of Nd ($Z = 60$) and Sm ($Z = 62$), while not in Ba ($Z = 56$) and Cs ($Z = 55$) ones [2]. Therefore, it is quite interesting how the change in the MSCR of Ce ($Z = 58$) isotopes behaves. Moreover, octupole deformation has been suggested for neutron-rich nuclei with $N \approx 88$ and $Z = 56 - 60$ [3]. In the case of Ce isotopes, alternating parity structure, which is an indicator of static octupole deformation, has been observed in ^{144,146}Ce but not in ^{148,150}Ce [4].

Gangrsky *et al.* measured the IS for atomic Ce stable isotopes by a laser-spectroscopic method [5]. As to radioactive isotopes, only the study by Fischer *et al.* with a conventional optical method was carried out for ^{144}Ce to determine the change in the MSCR [6]. As an extension of our previous study for Ce stable isotopes [7], we measured the IS for ^{144}Ce ($T_{1/2} = 284.9$ d) by collinear laser-ion-beam spectroscopy and determined the change in the MSCR.

Two types of samples were prepared in this work: a sample with natural abundance and a radioactive one. The isotope ^{144}Ce was prepared from the spent fuel of the JRR-3 reactor at the Japan Atomic Energy Research Institute. The purification of ^{144}Ce was carried out by using the solvent extraction technique to remove the other fission products and uranium. The total number of ^{144}Ce was found to be 6×10^{12} atoms by measuring γ rays with a Ge detector, which was consistent with the estimation from cumulative yield for the thermal neutron fission of ^{235}U.

The experimental setup is almost the same as our previous one [7]. A single-mode tunable dye laser with a wavemeter (Coherent 699-29) and rhodamine 110 dye was pumped by an Ar^+ laser (Coherent INNOVA-100-20). A part of the laser beam was used for the polarization spectroscopy of $^{127}I_2$ which provides an absolute frequency reference with a simple optical arrangement. A temperature-stabilized confocal Fabry-Pérot interferometer (FPI, Burleigh CFT-500) was used to calibrate the relative frequency of spectral lines. Each of the transmitted photons through either the FPI or the $^{127}I_2$ polarization spectrometer was detected by a photomultiplier tube (PMT, Hamamatsu R374). Ce ions were produced by a surface ionization ion source, accelerated to 40 keV, and mass separated by an analyzing magnet. The counterpropagating laser beam excited the Ce ions to the upper levels. The laser-induced fluorescence (LIF) was collected by an ellipsoidal mirror and detected by a cooled PMT (Hamamatsu R2256). Color glass filters suppressed stray light from the laser beam. The interaction region was defined with a cage kept at a constant potential of -3 kV, and accelerated ions were Doppler tuned to resonance with the laser frequency only inside the cage. The ion current was monitored by a Faraday cup and was typically 5 pA for ^{144}Ce. Signals from three PMT's were simultaneously counted during the laser frequency scanning, and recorded by multichannel scalers controlled by a personal computer.

The 534.93-nm transition from the $4f(^2F^0)5d^2(^1G)^2I^0_{11/2}$ level at 5969.01 cm^{-1} to the $4f5d(^1G^0)6p\ ^2H_{9/2}$ level at 24 663.05 cm^{-1} in Ce^+ [8] was measured in this work. The lower long-lived state at 5969.01 cm^{-1}, from which electric dipole transitions to much lower levels are allowed only with small transition probabilities, is thermally populated. Recently, the lifetime of the 24 663.05-cm^{-1} level has been measured by time-resolved LIF spectroscopy [9], and oscillator strengths of transitions in Ce^+ have been calculated theoretically [10]. According to these references, the 24 663.05-cm^{-1} level mostly decays to the levels near the ground state emitting the photon of wavelength about 440 nm.

The sample for the measurement of ^{144}Ce also contained stable ^{140}Ce and ^{142}Ce isotopes as fission products. Typical resonance peaks for the Ce isotopes together with the $^{127}I_2$ hyperfine structure (HFS) and the transmitted spectrum through the FPI are shown in Fig. 1. For each isotope, data were acquired from several scans, typically 15 GHz in width

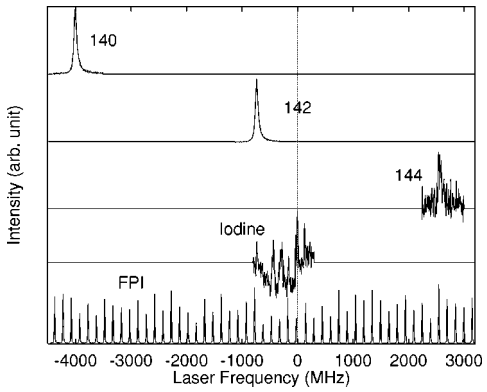

FIG. 1. Typical resonance peaks for the measured transition. Three upper spectra with mass numbers correspond to those of Ce^+. The second lowest spectrum is the $^{127}I_2$ HFS, and the lowest is transmitted spectrum through the FPI. These are simultaneously measured with each Ce spectrum. The horizontal positions of the Ce spectra are determined by referring to one of the $^{127}I_2$ HFS peaks and by using the spectrum of FPI.

and lasting 450 s each. The observed linewidths of the Ce and $^{127}I_2$ peaks were about 100 MHz and 10 MHz full width at half maximum, respectively. The former is mostly due to a ripple of the acceleration voltage. The relative frequency between each Ce peak and one of the $^{127}I_2$ HFS peaks was determined by comparison with the FPI spectrum. The observed shift in the peaks of the Ce spectra is due to a combination of IS and different Doppler shifts. To obtain the IS, the contribution of the Doppler shift was subtracted from the observed shift by measuring the acceleration voltage.

The experimental results of IS's for ^{144}Ce and stable isotopes are listed in Table I. The uncertainties include statistical and systematic errors. The latter come mainly from the accuracy for the measurement of the acceleration voltage ($\sim$2 MHz). The IS, which is a difference of the resonance frequency between isotopes, $\delta\nu_{i\mathrm{IS}}^{AA'}=\nu_{A'}-\nu_A$, is composed of the normal mass shift (NMS), the specific mass shift (SMS), and the field shift (FS):

$$\delta\nu_{i\mathrm{IS}}^{AA'}=\delta\nu_{i\mathrm{NMS}}^{AA'}+\delta\nu_{i\mathrm{SMS}}^{AA'}+\delta\nu_{i\mathrm{FS}}^{AA'}. \quad (1)$$

The NMS is calculated as $\delta\nu_{i\mathrm{NMS}}^{AA'}=\nu_A m(M_{A'}-M_A)/M_A M_{A'}$, where m and M_A are the masses of an electron and an ion with mass number A, respectively. The SMS can be theoretically evaluated only with limited precision. The FS, which is induced by the finite nuclear charge distribution, is written as [1]

$$\delta\nu_{i\mathrm{FS}}^{AA'}=E_i f(Z)\lambda, \quad (2)$$

TABLE I. Isotope shifts determined from the measurements in the 543.93-nm line of Ce^+ for radioactive ^{144}Ce and stable isotopes.

Isotope shifts (MHz)			
136–140	138–140	142–140	144–142
89.9(55)	26.0(42)	140.1(28)	108.5(89)

where E_i and $f(Z)$ are the electronic factor and the relativistic correction factor, respectively. The nuclear parameter λ gives changes in the MSCR and higher-order moments [11].

To estimate the contribution of the SMS to the observed IS, we performed a King-plot analysis, introducing the modified IS $\delta\nu_{i\mathrm{mod}}$ as

$$\delta\nu_{i\mathrm{mod}}^{AA'}=(\delta\nu_{i\mathrm{IS}}^{AA'}-\delta\nu_{i\mathrm{NMS}}^{AA'})\frac{M_A M_{A'}}{M_{A'}-M_A}\frac{M_{142}-M_{140}}{M_{140}M_{142}}. \quad (3)$$

The modified IS's of two transitions i and j are connected by the following linear equation:

$$\delta\nu_{i\mathrm{mod}}^{AA'}=\frac{E_i}{E_j}\delta\nu_{j\mathrm{mod}}^{AA'}+\delta\nu_{i\mathrm{SMS}}^{140,142}-\frac{E_i}{E_j}\delta\nu_{j\mathrm{SMS}}^{140,142}. \quad (4)$$

The slope of the King line E_i/E_j gives the ratio of the electronic factor of the FS, and the intercept corresponds to $\delta\nu_{i\mathrm{SMS}}^{140,142}-(E_i/E_j)\delta\nu_{j\mathrm{SMS}}^{140,142}$. The 446-nm transition in Ce^+ [12] was used as a reference line. A straight line was fitted to the data points for the stable isotopes because the IS of the 446-nm transition was measured only for the stable isotopes. Since the 446-nm transition corresponds to a pure $4f^2 6s$-$4f^2 6p$ transition, the SMS of this transition can be evaluated to be $\delta\nu_{j\mathrm{SMS}}=(0.3\pm0.9)\delta\nu_{j\mathrm{NMS}}$ [13]. Using this value, the FS and the SMS of the measured transition can be separated from the IS. Our results of the FS and SMS for the isotope pair ^{144}Ce-^{142}Ce are $\delta\nu_{i\mathrm{FS}}^{142,144}=157.5(102)$ MHz and $\delta\nu_{i\mathrm{SMS}}^{142,144}=-79.2(49)$ MHz, respectively.

Since the value of electronic factor E_j of the reference transition is known to be $E_j=-0.376(19)$ [5], the E_i of the measured transition can be obtained from the slope of the King line. The correction factor $f(Z)$ is derived from the isotope shift constant C_{unif} calculated by Blundell *et al.* [14] as $f(Z)=C_{\mathrm{unif}}/\lambda_{\mathrm{unif}}$ [15], where λ_{unif} is the nuclear parameter for the model nucleus of a uniformly charged sphere. Using Eq. (2), we obtained the λ. For Ce isotopes, the moments higher than $\langle r^2\rangle$ contribute about 4% to λ [16], and were taken into account. The value of $\delta\langle r^2\rangle^{142,144}$ was obtained to be

$$\delta\langle r^2\rangle^{142,144}=0.232(20)\ \ \mathrm{fm}^2. \quad (5)$$

There have been some experiments for Ce stable isotopes and ^{144}Ce to acquire the $\delta\langle r^2\rangle$. For comparison, we quote the previous value [13] $\delta\langle r^2\rangle^{142,144}=0.238(25)$ fm^2. The value of Ref. [13] was obtained by evaluating the result of a conventional optical study using a hollow cathode source [6] with the screening factor calculated by King and Wilson [17]. Since Aufmuth *et al.* [13] gave the λ, the correction of 4% from the higher-order moments is applied to their value. The values obtained in this work and the previous one are in good agreement within the errors. Figure 2 shows our experimental $\delta\langle r^2\rangle^{140,A}$ including those of stable isotopes for which the weighted averages are taken from our previous values [7] and the present ones.

A behavior of $\delta\langle r^2\rangle$ has been interpreted as the superposition of a difference in spherical nuclear charge radii and a change in the MSCR due to deformation, i.e.,

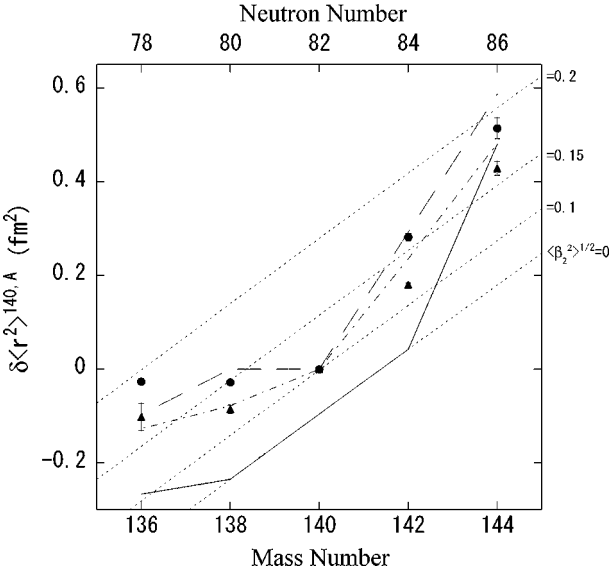

FIG. 2. Changes in the MSCR, $\delta\langle r^2\rangle^{140,A}$, for the Ce isotopes ($A=136$, 138, 142, and 144) from this work (circle). Those from the $B(E2)$ (triangle) together with the theoretical predictions of the FRDM (solid line), ETFSI (dashed line), and RMF (dash-dotted line) are also shown for comparison. The root-mean-square values of the quadrupole deformation parameter β_2 are indicated by parallel dotted lines, of which the gradients are given by the droplet model.

$$\delta\langle r^2\rangle=\delta\langle r^2\rangle_0+\frac{5}{4\pi}\langle r^2\rangle_0\delta\langle\beta_2^2\rangle, \tag{6}$$

where $\langle r^2\rangle_0$ is the MSCR of the corresponding spherical nucleus with the same volume and β_2 is the quadrupole deformation parameter. In Eq. (6) contributions from higher-order deformations are not taken into account. By using the droplet model of Myers *et al.* [18] to describe the contribution of the change in spherical shape, the root-mean-square quadrupole deformation parameters $\langle\beta_2^2\rangle^{1/2}$ were obtained from $\delta\langle r^2\rangle$ values. The results are shown by the parallel dotted lines in Fig. 2. Here, the droplet-model coefficients were quoted from Ref. [19]. In Fig. 2, the β_2 value of ^{140}Ce deduced from the reduced $E2$ transition probability $B(E2)$ by the formula [20]

$$\beta_2=\frac{4\pi}{3ZR_0^2}[B(E2)]^{1/2} \tag{7}$$

is assumed to be equal to the $\langle\beta_2^2\rangle^{1/2}$ value from the $\delta\langle r^2\rangle$, which is used as a reference point for the isodeformation lines. For comparison, Fig. 2 indicates the $\delta\langle r^2\rangle$ from the $B(E2)$ by using Eqs. (6) and (7). The β_2 values from $B(E2)$ are taken from Ref. [5] for ^{136}Ce and Ref. [20] for ^{140,142}Ce. The $B(E2)$ value for ^{138}Ce is a weighted average of 0.461(50) $e^2\,b^2$ [5] and 0.45(3) $e^2\,b^2$ [21], both of which were obtained from the measurements of the cross sections for Coulomb excitation. The β_2 for ^{144}Ce is deduced from the lifetime of the excited 2^+ level [22]. Also, Fig. 2 includes the theoretical predictions by the finite range droplet model (FRDM) [23], extended Thomas-Fermi and Strutinsky integral (ETFSI) [24], and the relativistic mean-field (RMF) theory [25]. Those of the FRDM were calculated by us using the deformation parameters given in Ref. [23].

At $N>82$, especially at $N=84$, discrepancies between the $\delta\langle r^2\rangle$ of this work and that of $B(E2)$ are larger than at $N<82$. In the $Z=56-60$ and $N\approx88$ region, a strong octupole correlation was anticipated theoretically [3]. From the FRDM, Möller *et al.* [23] predicted the octupole deformation parameter $\beta_3=-0.082$ for ^{144}Ce. By taking the higher-order deformation parameters of Ref. [23] into account, we can obtain a corrected $\delta\langle r^2\rangle$ value of 0.533 from the $B(E2)$. It agrees with the value from this work. However, there is the discrepancy at $N=84$ despite the expectation of much smaller deformations. Such a discrepancy also exists in the vicinity of neutron shell closures at $N=50$ and 126, and the influence of collective zero-point motion on the MSCR has been suggested [18]. To resolve such discrepancies and to deepen our understanding of the structures of Ce isotopes, it is strongly desired to extend this study to the more neutron-rich side including ^{146}Ce($N=88$) and ^{148}Ce($N=90$).

We would like to thank Prof. I. Endo at Hiroshima University for helpful discussions and encouragement.

[1] E. W. Otten, in *Treatise on Heavy-Ion Science*, edited by D. A. Bromley (Plenum, New York, 1989), Vol. 8, p. 515.
[2] J. Billowes and P. Campbell, J. Phys. G **21**, 707 (1995).
[3] W. Nazarewicz, P. Olanders, I. Rangnarsson, J. Dudek, G. A. Leander, P. Möller, and E. Ruchowska, Nucl. Phys. **A429**, 269 (1984).
[4] W. R. Phillips, R. V. F. Janssens, I. Ahmad, H. Emling, R. Holzmann, T. L. Khoo, and M. W. Drigert, Phys. Lett. B **212**, 402 (1988); S. J. Zhu *et al.*, *ibid.* **357**, 273 (1995).
[5] Yu. P. Gangrsky, S. G. Zemlyanoi, N. N. Kolensnikov, B. K. Kul'djanov, K. P. Marinova, B. N. Markov, V. S. Rostovskii, Yu. G. Teterev, Hoang Thi Kim Hue, and Chan Kong Tam, Yad. Fiz. **50**, 1217 (1989) [Sov. J. Nucl. Phys. **50**, 757 (1989)].
[6] W. Fischer, H. Hühnermann, K. Mandrek, Th. Meier, and D. C. Aumann, Physica C **79**, 105 (1975).
[7] Y. Ishida, H. Iimura, S. Ichikawa, and T. Horiguchi, J. Phys. B **30**, 2569 (1997).
[8] W. C. Martin, R. Zalubas, and L. Hagan, *Atomic Energy Levels: The Rare Earth Elements*, National Bureau of Standards circular (U.S. GPO, Washington, D.C., 1978).
[9] G. Langhans, W. Schade, and V. Helbig, Z. Phys. D **34**, 151 (1995).
[10] B. C. Fawcett, At. Data Nucl. Data Tables **46**, 217 (1990).
[11] E. C. Seltzer, Phys. Rev. **188**, 1916 (1969).
[12] R.-J. Champeau, Physica (Amsterdam) **62**, 209 (1972).
[13] P. Aufmuth, K. Heilig, and A. Steudel, At. Data Nucl. Data Tables **37**, 455 (1987).
[14] S. A. Blundell, P. E. G. Baird, C. W. P. Palmer, D. N. Stacey, G. K. Woodgate, and D. Zimmermann, Z. Phys. A **321**, 31 (1985).

[15] S. A. Ahmad, W. Klempt, R. Neugart, E. W. Otten, P.-G. Reinhard, G. Ulm, K. Wendt, and the ISOLDE Collaboration, Nucl. Phys. **A483**, 244 (1988).
[16] G. Torbohm, B. Fricke, and A. Rosén, Phys. Rev. A **31**, 2038 (1985).
[17] W. H. King and M. Wilson, Phys. Lett. **37A**, 109 (1971).
[18] W. D. Myers and W. J. Swiatecki, Nucl. Phys. **A336**, 267 (1980); W. D. Myers and K.-H. Schmidt, *ibid.* **A410**, 61 (1983).
[19] D. Berdichevsky and F. Tondeur, Z. Phys. A **322**, 141 (1985).
[20] S. Raman, C. H. Malarkey, W. T. Milner, C. W. Nestor, Jr., and P. H. Stelson, At. Data Nucl. Data Tables **36**, 1 (1987).
[21] G. Lo Bianco, K. P. Schmittgen, K. O. Zell, and P. v. Brentano, Z. Phys. A **332**, 103 (1989).
[22] M. Moszyński and H. Mach, Nucl. Instrum. Methods Phys. Res. A **277**, 407 (1989).
[23] P. Möller, J. R. Nix, W. D. Myers, and W. J. Swiatecki, At. Data Nucl. Data Tables **59**, 185 (1995).
[24] Y. Aboussir, J. M. Pearson, A. K. Dutta, and F. Tondeur, At. Data Nucl. Data Tables **61**, 127 (1995).
[25] G. A. Lalazissis, S. Raman, and P. Ring, At. Data Nucl. Data Tables (to be published).